

CHAPTER 196

WAVE IMPACT LOADING OF VERTICAL FACE STRUCTURES FOR DYNAMIC STABILITY ANALYSIS - PREDICTION FORMULAE -

P. Klammer¹, A. Kortenhaus², H. Oumeraci³

ABSTRACT

Based on impulse theory and experimental investigations on breaking wave kinematics and impact loads, prediction formulae for impact forces have been derived for vertical face breakwaters and further monolithic structures where wave effects dominate design considerations. Hydraulic model tests have been performed to obtain the water mass involved in the impact process and to verify the theoretical results obtained from theory.

INTRODUCTION

The results of the re-analysis of vertical breakwater failures (*Oumeraci, 1994*) have highlighted the importance of breaking waves and the subsequent destructive potential of impact loads. One of the principal lessons drawn from these failures consists in the urgent need to supplement the present static design approach by dynamic stability analysis. For this purpose, the impact loads induced by breaking waves on vertical breakwaters must be specified. It is the main purpose of this paper to develop an approach for the prediction of the impact load as needed for dynamic analysis of caisson breakwaters and further monolithic structures where wave effects dominate design considerations.

For this purpose, a formula for the impact force will be derived using impulse theory and solitary wave theory. Missing parameters were obtained from PIV measurements (particle image velocity) conducted at the University of Edinburgh. The obtained formulae will be compared to hydraulic model tests performed in the Large Wave Flume of Hannover (GWK).

¹Dipl.-Ing., Leichtweiß-Institut, TU Braunschweig, Beethovenstr. 51a, 38106 Braunschweig, Germany, e-mail: p.klammer@tu-bs.de

²Dipl.-Ing., Leichtweiß-Institut, TU Braunschweig, Beethovenstr. 51a, 38106 Braunschweig, Germany, e-mail: a.kortenhaus@tu-bs.de

³Prof. Dr.-Ing., Leichtweiß-Institut, TU Braunschweig, Beethovenstr. 51a, 38106 Braunschweig, Germany, e-mail: h.oumeraci@tu-bs.de

THEORETICAL BACKGROUND

A breaking wave impinging on a vertical wall generally induces impulsive pressures on the wall which are difficult to predict in terms of their magnitude as well as in terms of their spatial and temporal distribution (Fig. 1).

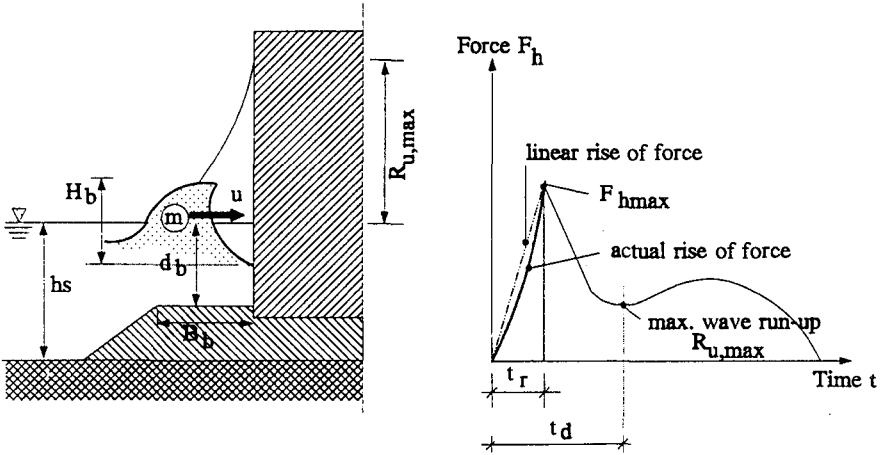


Fig. 1: Impact loading of vertical structure - definition sketch

The forward momentum of a fluid mass m hitting a wall with a horizontal velocity u will induce a force impulse (Fig. 1):

$$\int_0^{t_r} F_h(t) \cdot dt = m \cdot u \tag{1}$$

where t_r is the rise time up to the peak force $F_{h,max}$ and $F_h(t)$ is the horizontal force-time function. Assuming a linear temporal increase of the force $F(t)$, Eq. (1) yields:

$$\frac{1}{2} F_{h,max} \cdot t_r = m \cdot u \tag{2}$$

thus leading to the peak force:

$$F_{h,max} = 2 \cdot \frac{m \cdot u}{t_r} \tag{3}$$

Most of the difficulties encountered in applying Eq. (3) for the prediction of impact forces originate from the lack of information on the magnitude of the fluid mass m which is involved in the impact process and which accounts only for a small portion of the total mass M of the breaking wave impinging on the wall

$$m = k \cdot M \tag{4}$$

Assuming that the actual wave at breaking may be approximated by a solitary wave, its total mass M is given by the following relationship (Munk, 1949):

$$M = \rho \cdot \sqrt{\frac{16}{3} \cdot H_b \cdot d_b^3} \quad (5)$$

where ρ is the density of the fluid; H_b is the wave height at breaking and d_b is the water depth at the breaking point.

The maximum horizontal velocity approximates to (*Munk, 1949*):

$$u = \sqrt{g \cdot (d_b + H_b)} \quad (6)$$

and with the corresponding breaking criterion:

$$\frac{H_b}{d_b} = 0.78 \quad (7)$$

Eq. (6) yields:

$$u = \sqrt{g \cdot d_b \cdot (1 + 0.78)} \approx 1.33 \cdot \sqrt{g \cdot d_b} \quad (8)$$

and Eq. (5) yields:

$$M = \rho \cdot \sqrt{\frac{16}{3} \cdot H_b \cdot \left(\frac{H_b}{0.78}\right)^3} \approx 3.35 \cdot \rho \cdot H_b^2 \quad (9)$$

The forward momentum of the fluid mass m involved in the impact process is obtained from Eqs. (4), (8) and (9) to:

$$m \cdot u = (k \cdot M) \cdot u \approx 4.47 \cdot k \cdot \rho \cdot H_b^2 \cdot \sqrt{g \cdot d_b} \quad (10)$$

Considering Eq. (3) the dimensionless peak force is obtained as a function of the dimensionless rise time:

$$\frac{F_{h, \max}}{\rho \cdot g \cdot H_b^2} = k \cdot 8.94 \cdot \left(\frac{\sqrt{d_b/g}}{t_r} \right) = k \cdot 8.94 \cdot \left(\frac{t_r}{\sqrt{d_b/g}} \right)^{-1} \quad (11)$$

The nondimensional parameter k which represents the portion of the total mass of the breaking wave involved in the impact process has to be determined experimentally for each breaker type. According to *Bagnold (1938)* k is approximately 0.2. It can be concluded from Eq. (11) that the following issues will have to be further investigated:

- *Breaker types*: Breaker types have to be classified with respect to the loading induced in order to check the applicability of the proposed formula (impact loading and non impact loading)
- *Wave height H_b* : If H_b is not measured a method must be developed to determine the wave height at the breaker point taking into account the presence of the structure.
- *Mass parameter k* : for each loading case k has to be calculated from hydraulic model tests (see Eq. (4)).
- *Rise time t_r* : the determination of rise time t_r is dependent on the breaker type.

- *Occurrence frequency of relative horizontal force*: one of the two related parameters (relative horizontal force or relative rise time) in Eq. (11) must be taken from statistical analyses of hydraulic model tests.

(a) Typical Breaker Types

Model tests in the wave flume at the University of Edinburgh were conducted to experimentally define the water mass m involved in the impact process under different loading case conditions (Oumeraci *et al.*, 1995). In these tests velocity profiles for the following breaker types could be determined:

- well developed plunging breaker with large entrapped air-pocket
- plunging breaker with small entrapped air-pocket
- "flip-through" breaker

A rough classification of wave loading is given in Fig. 2 which distinguishes between 'pulsating' loads and impact loads. For the latter which is induced by waves plunging on the structure the Goda method (Goda, 1985) is not applicable (Takahashi *et al.*, 1993). The proposed method was therefore developed for this type of loading (Fig. 2c).

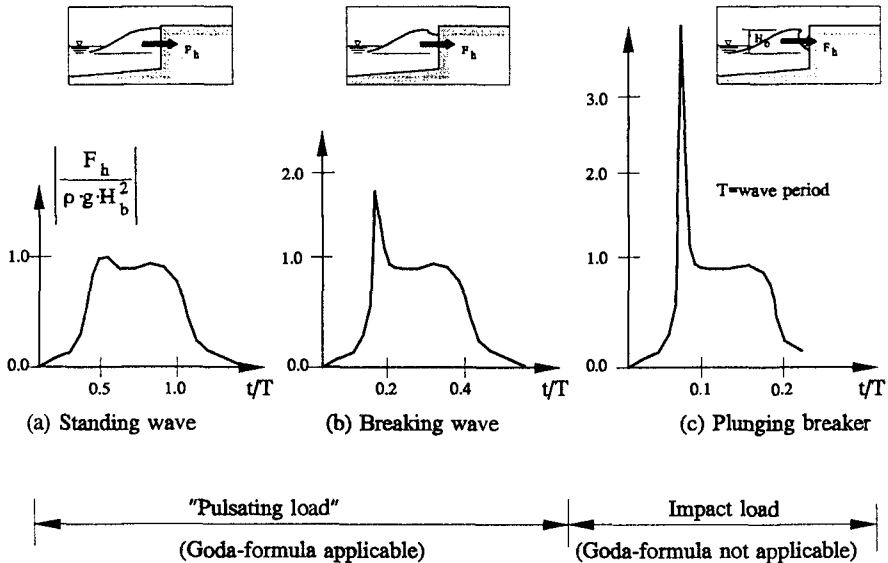


Fig. 2: Classification of wave loading

(b) Estimation of Incident Wave Heights

Wave breaking can be taken into account by a formula given in Oumeraci *et al.*, 1993 in which the total reflection of the structure and its influence on wave breaking is considered:

$$H_b = L_b \cdot \left[0.1025 + 0.0217 \left(\frac{1 - C_r}{1 + C_r} \right) \right] \cdot \tanh \left(2 \pi \frac{d_b}{L_b} \right) \quad (12)$$

In Eq. (12) d_b is the water depth at the breaking point of the wave, L_b is the wave length of the breaking wave and C_r is the reflection coefficient of the structure. The significant wave height can be calculated by a comparison between H_d (calculated from shoaling) and H_b in which H_d may not exceed H_b .

The water depth in front of the structure can be regarded as the governing parameter for the magnitude of the resulting wave height H_b . It can be assumed that a relatively short berm in front of the structure ($B_b/L \leq 0.15$) will have only a small influence on wave breaking. Therefore, it would not be correct to use the water depth d in front of the structure as an input ($d = d_b$) for Eq. (12). On the other hand using the water depth hs (Fig. 1) at the toe of the berm would certainly overestimate the breaker height as the influence of the berm on the breaking would be neglected. It is assumed that the berm width B_b , the wave length L and the slope of the berm 1:m ($m = \cot \alpha$) will influence the breaking of waves. Therefore an effective water depth d_m can be derived which takes into account the aforementioned parameters (Fig. 1):

$$d_m = d + B_{rel} \cdot m_{rel} \cdot (hs - d) \quad (13)$$

In Eq. (13) B_{rel} is the part of the berm width which influences the effective water depth:

$$B_{rel} = \begin{cases} 1 & \text{for } B_b/L > 1 \\ 1 - 0.5 \cdot B_b/L & \text{for } B_b/L \leq 1 \end{cases} \quad (14)$$

The parameter m_{rel} in Eq. (13) is a part of the slope of the berm which influences the effective water depth and is assumed to be:

$$m_{rel} = \begin{cases} 1 & \text{for } m < 1 \\ m^{-0.5} & \text{for } m \geq 1 \end{cases} \quad (15)$$

For solitary waves the effective water depth d_m is very close to the depth hs ($d_m = hs$), so that $B_{rel} = 1$ and $m_{rel} = 1$. This is confirmed by comparing the calculated wave height using Eq. (12) and this assumption with measurements in the Large Wave Flume of Hannover (GWK) (Fig. 3).

A relatively good agreement between measured and calculated values is also obtained for regular and random wave tests.

(c) Experimental Determination of Mass Parameter k

The basic concept for the evaluation of water mass m involved in the impact process is illustrated in Fig. 4. The impulse of a water mass m with a horizontal velocity $v(z)$ at a height z above the berm can be calculated as follows (Fig. 4a):

$$v(z) \cdot dm(z) = v(z) \cdot [\rho \cdot l(z) \cdot dz] \quad (16)$$

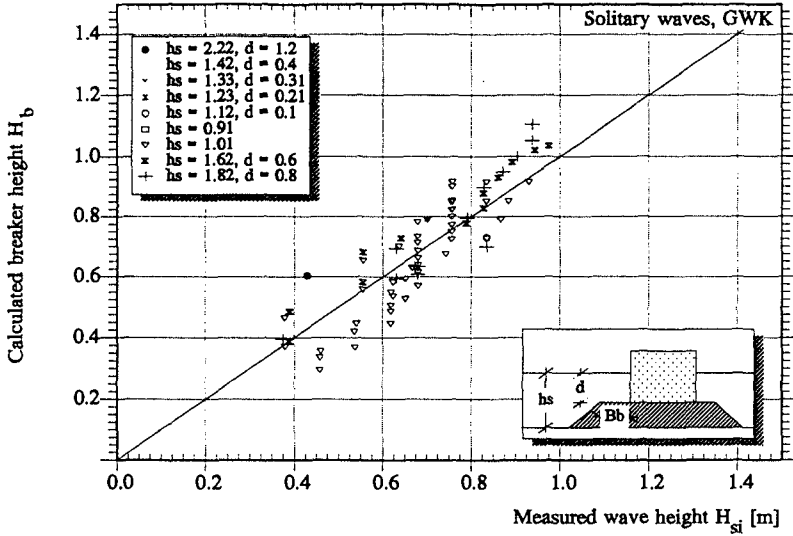


Fig. 3: Calculated vs measured wave height H_b for solitary waves

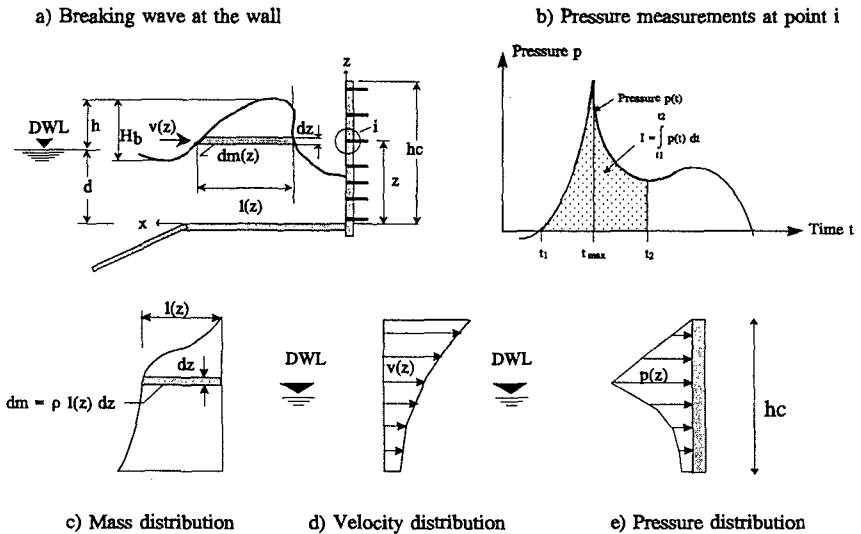


Fig. 4: Principal determination of wave induced loading

The vertical component of the velocity can be neglected. This impulse (Eq. (16)) is equal to the pressure impulse $dI = p(t) \cdot dt$ at the wall measured at a height z above the berm during the period t_1 to t_2 (Fig. 4b):

$$p(t) \cdot dt = [\rho \cdot l(z) \cdot dz] \cdot v(z) \tag{17}$$

Both the velocity (Fig. 4d) and the pressure distribution (Fig. 4e) were measured over the full height of the wall. From those, it is possible to determine the mass distribution for the respective breaker type (Fig. 4c).

The calculation of water masses involved in the impact process was performed according to the height of the pressure cells 6-12 at seven locations (Fig. 4a). The measured pressure distributions were integrated from time t_1 to the time of the maximum t_{max} (Fig. 4b) and from time t_1 to the time of maximum wave run-up at the wall t_2 (Fig. 4b). These values were multiplied by the horizontal velocities obtained from the PIV measurements.

Finally, the mass parameter k could be estimated for different breaker types (Tab. 1) (see also Fig. 4):

Tab. 1: Mass parameter and impulse ratio for different breaker types

Loading case	Breaker type	Mass parameter k [%]	Impulse ratio ^{*)} I_{rFh}/I_{dFh} [%]
2	Well developed plunging breaker with much air enclosed	11	9
3	Plunging breaker with little air enclosed	16	15
4	flip-through breaker	28	21

*) I_{rFh}, I_{dFh} : definition see Fig. 4

In Tab. 1 the experimentally determined mass parameter k (11-28%) are in the same order of magnitude as the average value $k \approx 0.2$ proposed by *Bagnold (1938)*.

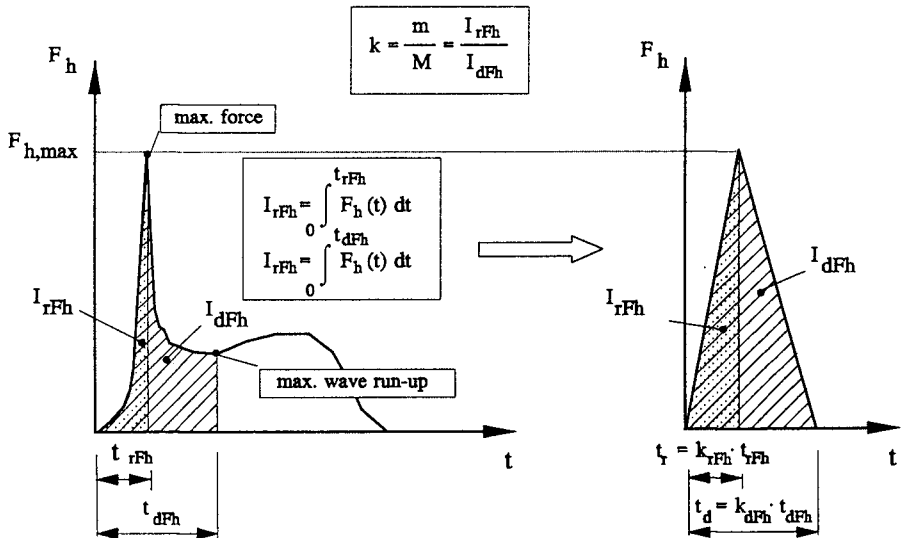


Fig. 5: Substitution of the real force history by an equivalent triangular force

Fig. 5 (left side) illustrates a typical horizontal force history induced by a wave impinging on the wall. The maximum load is reached after a time t_{rFh} and the maximum wave run-up after a time t_{dFh} . At that time it is assumed that the total mass M of the breaking wave has transferred its impulse I_{dFh} to the wall whereas the mass m inducing the impact transfers its impulse I_{rFh} to the wall over a duration t_{rFh} . Subsequently, the mass parameter k can be verified by the ratio of I_{rFh} and I_{dFh} as given in Fig. 5.

This force impulse ratio calculated for the same PIV tests as those used for the determination of k leads to results also given in Tab. 1. A comparison between the values of the PIV tests and the impulse ratio clearly shows that the latter are slightly smaller.

(d) Temporal Development of Horizontal Force

The theoretical approach is based on the assumption of a linear rise of the horizontal force to the maximum load (Fig. 5). Actually the shape of this force increase is strongly dependent on the breaker types.

Therefore two factors k_{rFh} and k_{dFh} are introduced which account for the different geometries of load histories in the case of breaking waves. The factor k_{rFh} is the value that has to be multiplied with the rise time t_{rFh} in order to obtain a triangle with the same area (force impulse). For the horizontal force this can be calculated as follows (Fig. 4):

$$k_{rFh} = \frac{2 \cdot I_{rFh}}{F_{h, \max} \cdot t_{rFh}} \quad \text{with } k_{rFh} < 1 \quad (18)$$

For k_{dFh} a similar approach yields:

$$k_{dFh} = \frac{2 \cdot \Delta I_{dFh}}{F_{h, \max} \cdot \Delta t_{dFh}} \quad \text{with } k_{dFh} < 1 \quad (19)$$

where the portion of impulse ΔI_{dFh} is defined as:

$$\Delta I_{dFh} = \int_{t_{rFh}}^{t_{dFh}} F_h(t) dt \quad (20)$$

(e) Prediction Formula for Impact Loading of Vertical Structures

Using the results derived in the previous sections Eq. (11) may be rewritten as:

$$\frac{F_{h, \max}}{\rho \cdot g \cdot H_b^2} = 8.94 \cdot \frac{k}{k_{r, Fh}} \cdot \left(\frac{t_r}{\sqrt{d_b/g}} \right)^{-1} \quad (21)$$

where k and $k_{r, Fh}$ are obtained from PIV tests:

- well developed plunging breaker: $k = 0.10$; $k_{r, Fh} = 0.80$
- plunging breaker: $k = 0.15$; $k_{r, Fh} = 0.80$
- 'flip-through': $k = 0.20$; $k_{r, Fh} = 1.00$

Since a distinction between these three loading cases based on simple parameter analysis is not yet available it is proposed to select a conservative value for $k = 0.20$ and $k_{r, Fh} = 0.80$, thus resulting in the following prediction formula:

$$\frac{F_{h,\max}}{\rho \cdot g \cdot H_b^2} = 2.24 \cdot \left(\frac{t_r}{\sqrt{d_b/g}} \right)^{-1} \quad (22)$$

This prediction formula can be compared with measurements obtained from GWK tests (Fig. 6) which are described in more detail in *Kortenhaus et al. (1994)*.

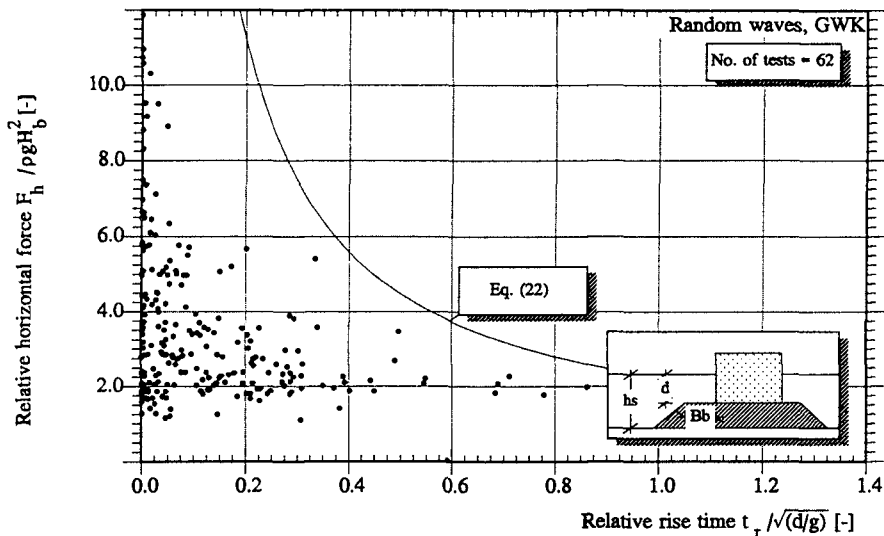


Fig. 6: Comparison of prediction formula to large-scale measurements (random waves)

It can be seen from Fig. 6 that the prediction formula in Eq. (22) represents approximately the upper envelope to the random wave test results. This was to be expected as a conservative approach was used where solitary wave theory was used. Therefore, for solitary waves the prediction formula better fits the data obtained from the model tests (Fig. 7). However, the large scatter in the data can be explained as follows:

- breaking processes at a vertical wall are extremely stochastic which can only be approximated by the aforementioned approach;
- the sampling frequency of the pressure transducers used in the tests was not high enough leading to errors in both defining the rise time and the maximum load;
- sampling noise during the measurements cause some problems in defining the zero crossings which are essential in defining the accurate rise times.

The relation between rise time t_r and total duration t_d of the load (both for triangular load geometries) can also be taken from large-scale measurements:

$$t_d = t_r + 0,35 \cdot \left(1 - \exp(-20 \cdot t_r) \right) \quad (23)$$

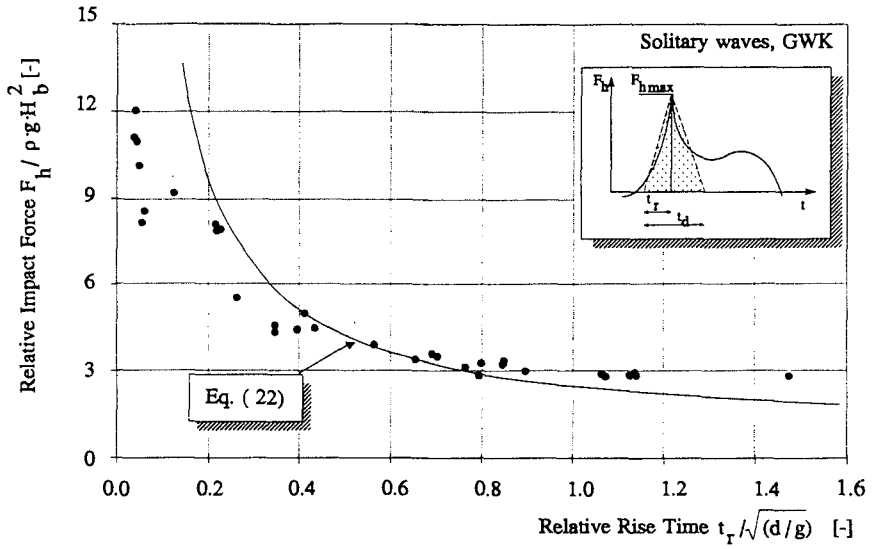


Fig. 7: Comparison of prediction formula to large-scale measurements (solitary waves)

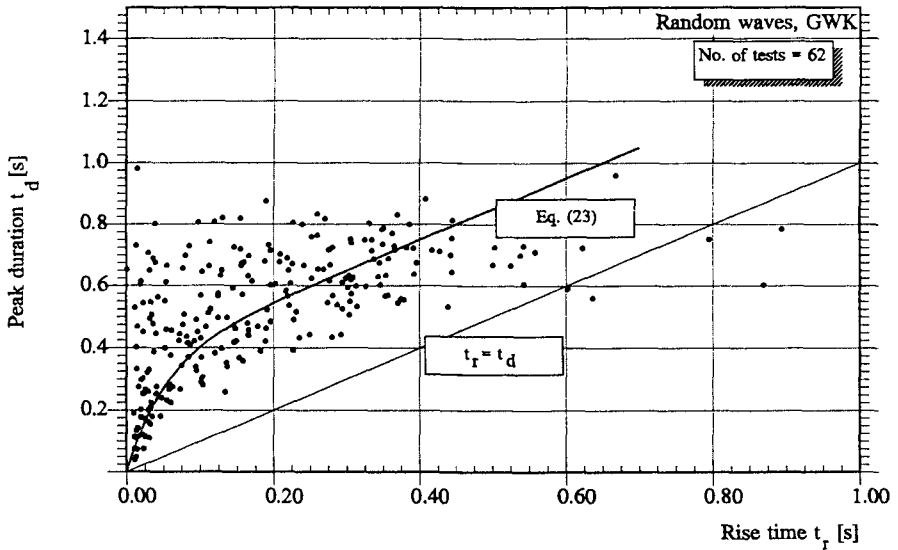


Fig. 8: Total duration t_d vs rise time t_r for random waves in large-scale model tests

(f) Statistical Distribution for Relative Horizontal Forces

In order to apply the prediction formula (Eq. (22)) a statistical distribution function for relative horizontal forces $F_h / \rho \cdot g \cdot H_b^2$ is needed. Such a distribution function has been developed by modifying the standard Weibull distribution (Weibull, 1951) as follows:

$$F(x) = 1 - \exp\left[-\gamma \cdot (\ln x - \beta)\right]^\alpha \quad x > 0 \tag{24}$$

In Eq. (24) α , β and γ are the parameters of the modified Weibull functions where $F(x)$ is the distribution function. Fig. 9 shows the non exceedance probabilities of relative horizontal forces taken from large-scale measurements with random waves.

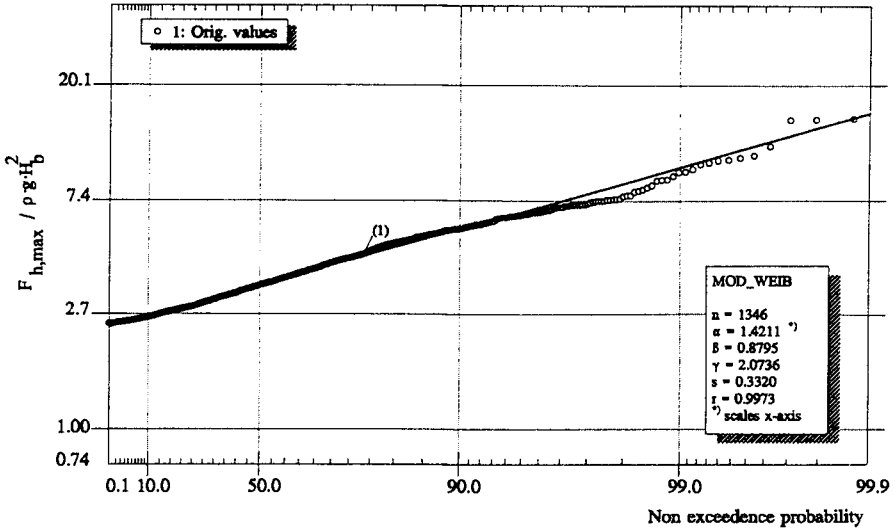


Fig. 9: Statistical distribution function of relative horizontal forces

Assuming a non exceedance value a relative horizontal force can be read from Fig. 9 or calculated by Eq. (24). In this approach no scale effects are considered but will have to be investigated further.

(g) Temporal Development of Pressure Distribution

For dynamic analyses it is very often necessary to apply pressure distributions at the front face of the structure instead of horizontal forces. Therefore, a pressure distribution has to be suggested. In Fig. 10 the temporal development of a typical pressure distribution for a well developed plunging breaker is shown over 30 time steps with the maximum impact force indicated in the centre of the figure.

It can be seen from Fig. 10 that the pressure distribution changes its shape significantly with time. Furthermore, the peak pressure close to the design water level (DWL) is very high at the time of the maximum force. As a result of the analysis of several distributions similar to that shown in Fig. 10 a very simplified pressure distribution at the time of peak force occurrence is proposed for design purposes in Fig. 11.

In Fig. 11 the height of the pressure distribution η^* above DWL is dependent on the wave height H_b and can be derived as follows:

$$\eta^* = 0.8 \cdot H_b \tag{25}$$

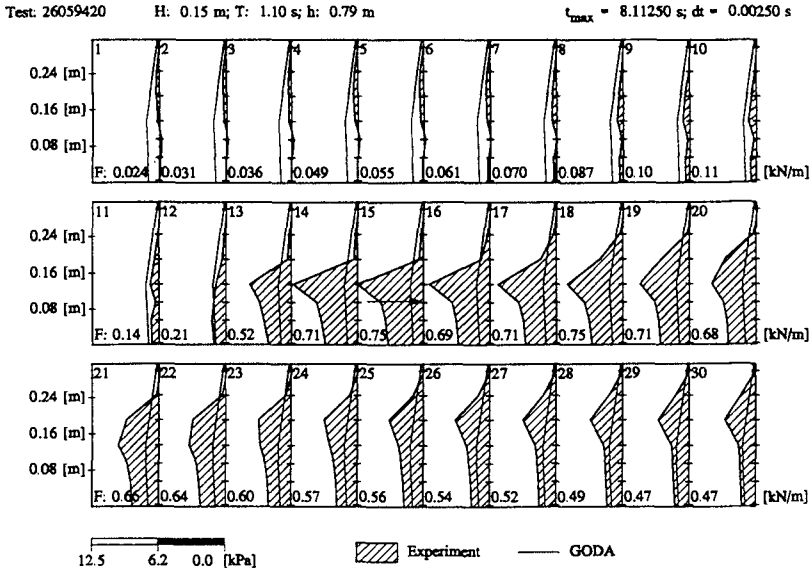


Fig. 10: Pressure distribution for a 'well developed plunging breaker'

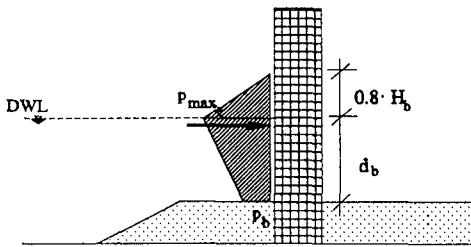


Fig. 11: Pressure distribution for breaking waves

In Eq. (25) H_b is the wave height of the breaking wave which can be taken from Eq. (12). The pressure head at the berm p_b can be approximated by:

$$p_b = 0.45 \cdot p_{max} \tag{26}$$

where p_{max} is the pressure at DWL. Therefore, p_{max} can be calculated from the horizontal force history by:

$$p_{max}(t) = \frac{F_h(t)}{0.4 d_b + 0.3 d_b + 0.4 H_b} = \frac{F_h(t)}{0.7 d_b + 0.4 H_b} \tag{27}$$

(h) Dynamic Load Factor

For practical design it might be desirable to use a static approach. This can be obtained by assuming an equivalent static load inducing the same response of the structure. The ratio between equivalent static and dynamic load, called dynamic load factor D, must be determined (*Oumeraci and Kortenhaus, 1994*).

DESIGN CONCEPT

For breaking waves at a structure prediction formulae have been developed in the previous sections. Therefore, an overall deterministic design concept can be derived which is principally summarized in Fig. 12.

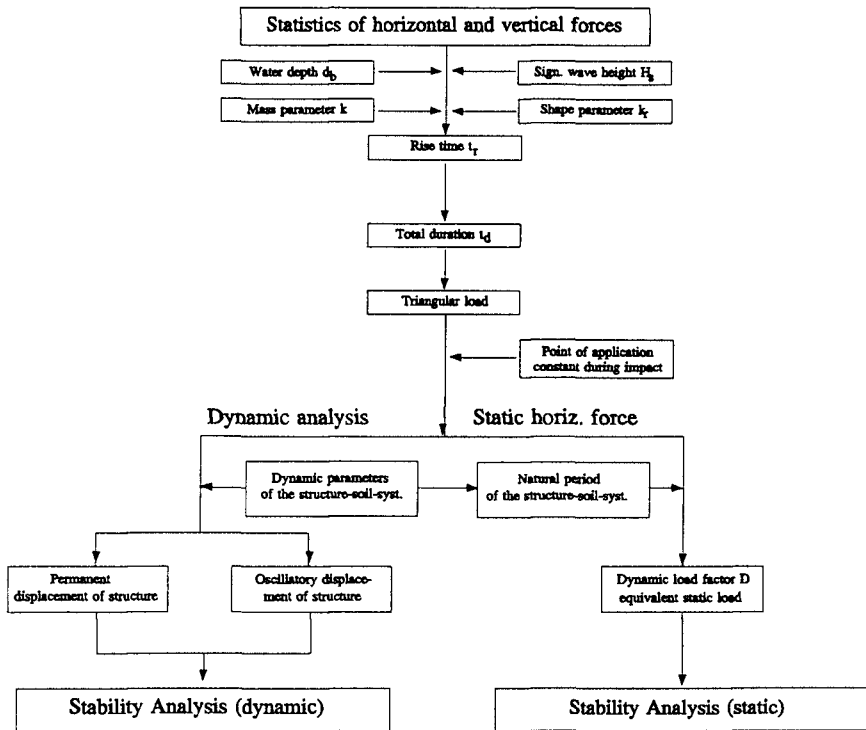


Fig. 12: Design concept for breaking wave loads

CONCLUDING REMARKS AND FUTURE WORK

Based on impulse theory and experimental investigations on breaking wave kinematics and impact loads, prediction formulae for impact forces have been derived for vertical face breakwaters.

Hydraulic model tests have been performed to assess the water mass involved in the impact process and to verify the results obtained from theory. It was found that the proposed formula represents the upper envelope of the measured values.

The ongoing and future research work is directed towards further improvement of the proposed prediction formulae. This will be particularly achieved by a better definition of the mass parameter k and of the pressure distribution for each breaker type. Moreover, a similar approach will also be developed for the uplift pressures and forces induced by breaking waves.

ACKNOWLEDGEMENTS

This study was supported by the German Research Council (DFG), Bonn. Additional support is provided by the European Union within the Research Programme MAST III (PROVERBS, contract no. MAS3-CT95-0041).

REFERENCES

- BAGNOLD, R.A. (1938): Interim Report on Wave-Pressure Research. *Journal of the Institution of Civil Engineers (ICE)*, vol. 12, pp. 202-226.
- GODA, Y. (1985): Random seas and design of maritime structures. Tokyo: University of Tokyo Press, 323 pp.
- KORTENHAUS, A.; OUMERACI, H.; KOHLHASE, S.; KLAMMER, P. (1994): Wave-induced uplift loading of caisson breakwaters. *Proceedings International Conference Coastal Engineering (ICCE)*, ASCE, Kobe, Japan, vol. 24, Part 2, pp. 1298-1311.
- MUNK, W.H. (1949): The solitary wave theory and its application to surf problems. *Annals of the New York Academy of Sciences*, pp. 378-424.
- OUMERACI, H.; KLAMMER, P.; PARTENSCKY, H.-W. (1993): Classification of breaking wave loads on vertical structures. *Journal of Waterway, Port, Coastal and Ocean Engineering*, ASCE, vol. 119, no. WW4, pp. 381-397.
- OUMERACI, H. (1994): Review and analysis of vertical breakwater failures - lessons learned. *Coastal Engineering, Special Issue on 'Vertical Breakwaters'*, Amsterdam, The Netherlands: Elsevier Science Publishers B.V., vol. 22, nos. 1/2, pp. 3-29.
- OUMERACI, H.; KORTENHAUS, A. (1994): Analysis of dynamic response of caisson breakwaters. *Coastal Engineering, Special Issue on 'Vertical Breakwaters'*, Oumeraci, H. et al., Amsterdam, The Netherlands: Elsevier Science Publishers B.V., vol. 22, nos. 1/2, pp. 159-183.
- OUMERACI, H.; BRUCE, T.; KLAMMER, P.; EASSON, W.J. (1995): Breaking wave kinematics and impact loading of caisson breakwaters. *Proceedings International Conference on Coastal and Port Engineering in Developing Countries (COPEDEC)*, Rio de Janeiro, Brazil, vol. 4, Part 3, pp. 2394-2410.
- OUMERACI, H.; KORTENHAUS, A.; KLAMMER, P. (1995): Displacement of caisson breakwaters induced by breaking wave impacts. *Proceedings of the Conference on Coastal Structures and Breakwaters*, ICE, London, U.K.: Thomas Telford Ltd.
- TAKAHASHI, S.; TANIMOTO, K.; SHIMOSAKO, K.-I. (1993): Experimental study of impulsive pressures on composite breakwaters. *Report. Port and Harbour Research Institute (PHRI)*, vol. 31, no. 5, Tokyo, Japan, pp. 33-72.
- WEIBULL, W. (1951): A statistical distribution function of wide applicability. *Journal of Applied Mechanics*, vol. 18, pp. 293-297.